CrossMark

ORIGINAL PAPER

A nonlinear contact pressure distribution model for wear calculation of planar revolute joint with clearance

Aibin Zhu · Shengli He · Jianwei Zhao · Wencheng Luo

Abstract As various errors result from manufacture and assembly processes or wear effect, clearance joint widely exists in mechanical system as a base component. The coupling analysis of tribology and dynamics of clearance joint is important to the reliability of mechanical system. A nonlinear contact pressure distribution mode (NLCP) is proposed to combine dynamics analysis with wear calculation together in this paper. The discrete thought of Winkler model is adopted to deal with contact problem with a high conformal rate. The contact relationship in a local microcontact area can be regarded as the contact between cylinder and plane. And the local contact pressure is acquired based on Hertz contact theory. The NLCP model has not only described the nonlinear relationship between contact pressure and penetration depth, but also avoided the complexity in contact pressure computation. The performance of NLCP model is demonstrated in comparison with asymmetric Winkler model, revealing that NLCP model has enhanced the calculation accuracy with a good efficiency. A comprehensive experimental study on the wear calculation of a slider–crank mecha-
nism with clearance joint is presented and discussed to provide an experimental verification for NLCP model. The paper's work has solved the contact problem with a high conformal rate and has described the nonlinear relationship between contact pressure and penetration depth. It has great value to the wear analysis of clearance joint.

Keywords Clearance joint · Contact pressure calculation · NLCP model · Wear calculation

1 Introduction

As an inevitable factor in kinematic joints, joint clearance has a heavy effect on the dynamics performance of mechanical system. It is known to be the source for impact forces. These forces not only create increased vibration and noise, but also reduce system reliability, stability, life and precision [1]. In order to efficiently evaluate the contact–impact force resulting from collisions in multi-body systems, special attention must be given to the numerical description of contact pressure distribution model. Over the last few years, extensive work has been done to study the effects of clearance on the dynamic response and wear behavior of mechanical system [2–4]. And lots of analysis models have been proposed [5–8]. Yaqubi et al. [9] have investigated the effects of joint friction on dynamical behavior and nonlinear response of the mechanism. Varedi-Koulaei et al. [10] have presented an optimization algo-

A. Zhu (✉) · S. He · W. Luo
Key Laboratory of Education Ministry for Modern Design and Rotor-Bearing System, Xi'an Jiaotong University, 28 Xianning West Road, Xi'an 710049, China
e-mail: abzhu@mail.xjtu.edu.cn

J. Zhao
School of Mechanical Electronic and Information Engineering, China University of Mining and Technology (Beijing), Beijing 100083, China

rithm to improve the performance and the accuracy of the manipulator with clearance. Askari et al. [11] have modeled the ceramic-on-ceramic (CoC) hip prosthesis with clearance, and the effects of friction, hip implant size and the head initial position were analyzed. As the clearance joint widely exists in mechanical system as a base component, it is meaningful to perform the coupling analysis of tribology and dynamics. Therefore, as one of the most important contents for wear calculation, the research of contact pressure distribution of clearance joint is necessary and can build a bond between dynamics analysis and wear calculation.

The traditional contact pressure computation is mostly based on the classic Hertz contact theory [12]. The Hertz contact theory lays the foundation for almost all of the available force models, but it is not appropriate for most impacts in practice [13]. For one thing, Hertz contact theory exhibits the same restrictions, which prevent them from being used with conformal contact conditions often observed for small clearance. For another, Hertz contact theory does not account for the energy dissipation during the contact–impact process, so it cannot be used during both phases of contact, namely the loading and unloading phases [14]. Afterward, many contact force calculation models are presented based on Hertz contact theory considering the energy dissipation, such as Hunt–Crossley model [15], Herbert and McWannell model [16]. It is worth mentioning that Lankarani–Nikravesh model (L–N) [17,18] is frequently applied to calculate the contact force. Information on the impact velocity, material properties of the colliding bodies and geometry characteristics of the contact surfaces are all taken into consideration in this contact force model [17]. These characteristics are observed through a continuous function of penetration depth and contact force. Bai and Zhao [19] presented a new contact force model of clearance joint for planar mechanical systems based on L–N model. Muvengei et al. [20] studied the behavior of planar rigid-body mechanical systems due to the dynamic interaction of multiple clearance joints, and L–N model was adopted to describe the normal forces in clearance joints. Zhang et al. [21] combined Newton–Euler equations with L–N model to establish the dynamic equations of a 3-DOF parallel mechanism with clearance joints. The penetration depth is described as an implicit function of the contact force in these models. Consequently, a numerical iterative technique is required to evaluate the contact force for a given penetration depth. In a dynamic

analysis code, it is implied that the iterative process for the solution of nonlinear equations has to be solved at each integration time step [22]. The complicated solving processes of strong nonlinear differential equations pose some limitations in their use.

In order to solve the high conformal contact problem and avoid the complexity of contact pressure calculation, Winkler surface model is widely adopted to calculate the contact pressure of clearance joint. Flodin and Andersson [23] used the Winkler surface model to predict surface behavior and wear condition. Põdra and Andersson [24] studied the advantages and disadvantages of using the simple Winkler surface model in wear simulation. Wear simulations had been made with a Winkler surface model and compared with simulations made with an FEM model. The results show a very good agreement. Liu et al. [25] developed an approximate model for the contact problem of cylindrical joints with clearances through modeling the pin as a rigid wedge and the elastic plate as a simple Winkler elastic foundation. The approximate model provided a more direct and effective formula to describe the properties of the contact in the cylindrical joint with clearances. Su et al. [26] used Winkler surface model to calculate joints reaction and contact pressure. Li et al. [27] presented an unsymmetrical Winkler surface model and a double elastic layer Winkler model, which turn out to be a good result. However, in the actual contact process, the relationship between contact pressure and penetration is nonlinear. Thus, a simple linearization relationship is not rigorous to describe contact pressure and penetration depth in Winkler model.

The tribology and dynamics behaviors of mechanical system relate to each other closely in engineering applications. Considering the limitation of traditional contact force calculation model and Winkler model, the NLCP model is proposed based on the discrete thought of Winkler model, and the local contact pressure is acquired based on Hertz contact theory. The performance of NLCP model is demonstrated in comparison with asymmetric Winkler model, revealing that NLCP model has enhanced the calculation accuracy with a good efficiency. A comprehensive experimental study on the wear calculation of a slider–crank mechanism with clearance joint is presented and discussed to provide an experimental verification for NLCP model. The NLCP model has not only described the nonlinear relationship between contact pressure and penetration depth, but also avoided the complexity in contact
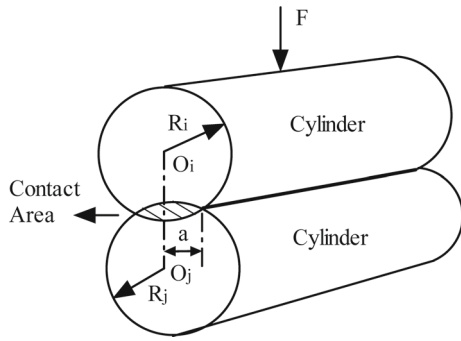
Fig. 1 Hertz contact force model

pressure computation. The paper's work has solved the contact problem with a high conformal rate and has described the nonlinear relationship between contact pressure and penetration depth.

2 Demonstration of contact pressure calculation model

2.1 Hertz contact force model

Hertz contact theory is a pure elastic contact model based on entirely elastic deformation [13,22]. The great advantage of the Hertz law compared with Kelvin–Voigt contact model is its nonlinearity [28]. It mainly demonstrates the quasi-static contact problem of elastomer, such as the cylindrical contact pressure calculation, as shown in Fig. 1. It is a nonlinear contact pressure calculation model. The relationship between contact force and penetration depth is as follows [29].

$$F = K\delta^n \tag{1}$$

where F—contact force and δ—relative penetration depth.

K is the contact stiffness coefficient, determined by the material properties and the shape of the contact surfaces. For two spheres in contact, the generalized stiffness coefficient is the function of the radii of the both spheres and the material properties [30].

$$K = \frac{4}{3\pi(\sigma_i + \sigma_j)}\left[R_i R_j / \left(R_i - R_j\right)\right]^{\frac{1}{2}} \tag{2}$$

$$\begin{cases} \sigma_i = (1 - v_i^2)/(\pi E_i) \\ \sigma_j = (1 - v_j^2)/(\pi E_j) \end{cases} \tag{3}$$

R_i, R_j are the radius of curvature. For the contact between a cylinder body i and a plane surface body

j, $R_j = \infty$. E_i, E_j are the elastic modulus of contact elements, and v_i, v_j are the Poisson's ratio of contact elements.

2.2 Traditional Winkler model

The Winkler surface model takes discrete thoughts to deal with contact problem. It can be well applied to the contact pressure calculation of high conformal contact. Thus, the contact pressure calculated by this model has a better accuracy than the result computed by Hertz contact theory [25]. The relationship between contact pressure and penetration depth is described as follows [24].

$$p_i = \frac{E_w}{L_i}\delta_i \tag{4}$$

where p_i—contact pressure; E_w—complex elastic modulus; and L_i—thickness of elastic layer. It is generally assumed that plastic deformation does not occur to the bushing under light load, and then the L_i is regarded as the thickness of the bushing, and δ_i, the relative penetration depth.

The external load can be acquired via summating the forces of all the springs on contact surface [26].

$$F_{\text{total}} = \sum_{i=1}^{n} p_i A_i \cos\beta_i \tag{5}$$

where F_{total}—total pressure of all the springs; A_i—contact area at the ith spring; β_i—angle between the ith spring and external load; and n—total spring number in contact area.

As shown in Fig. 2, the penetration area of clearance joint is $C_1 C_2$. The bushing is regarded as the elastic foundation. The contact is discretized as the contact of a series of springs. In the contact area, F_{total} is equal to F_N.

2.3 Asymmetric Winkler model

Winkler model, compared with other contact pressure calculation models, has higher computation efficiency with good accuracy [24,25]. However, the contour of clearance joint is regarded as an ideal circle in traditional Winkler model, which is incorrect because of the wear behavior happening to the clearance joint. Therefore, an asymmetric Winkler model is presented. The
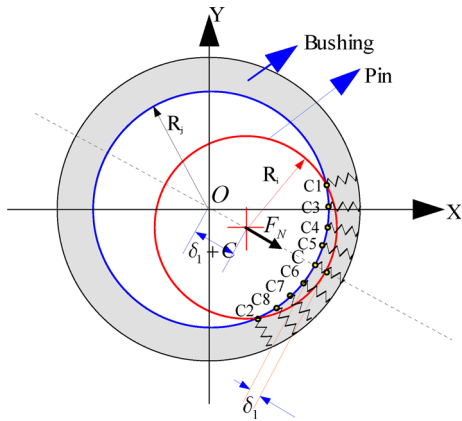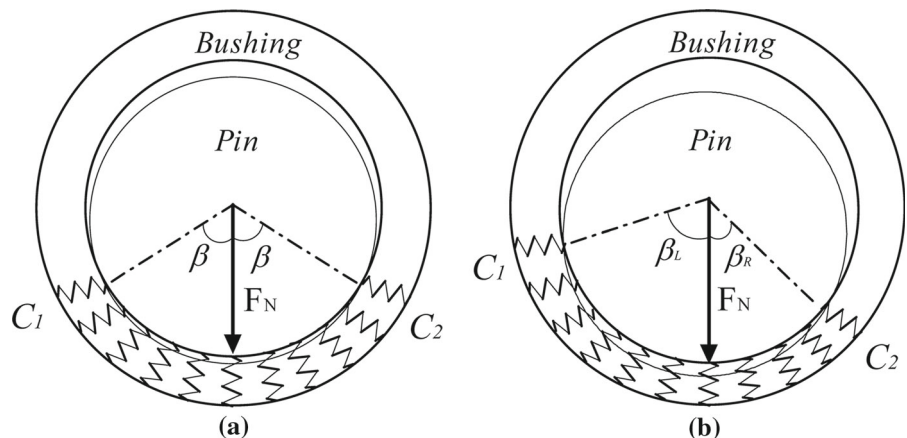
Fig. 2 Winkler surface model applied to clearance joint

comparison between Winkler model and asymmetric Winkler model is shown in Fig. 3.

From Fig. 3a, we can see that when there is a concentrated force F_N on the bushing, the deformation springs on both sides are symmetric distribution in traditional Winkler model. But in fact, the bushing inside contour changes with the effect of wear. Thus, the deformation springs on both sides are asymmetric distribution, as shown in Fig. 3b. The number of deformation springs on each side should be counted separately in asymmetric Winkler model. According to the boundary conditions of deformation edge, there will be a triangle with the vertices of pin center, bushing center and critical point of contact. Then, the discrete geometry data of pin surface and bushing inner surface are taken to calculate the number of deformation springs on both sides.

$$N = N_{\mathrm{L}} + N_{\mathrm{R}} \qquad (6)$$

where N—the total deformation spring number; N_{L}—the deformation spring number on the left side; and N_{R}—the deformation spring number on the right side.
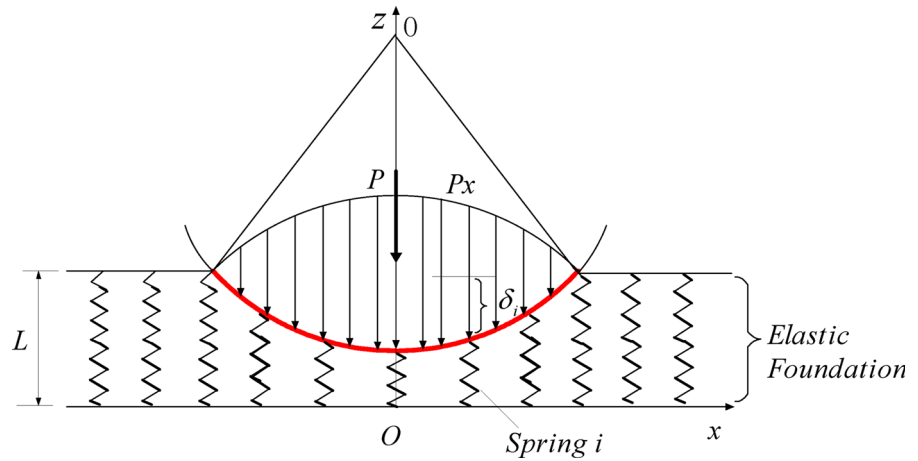
2.4 NLCP model

On the one hand, based on the discrete thought, the Winkler model is no longer restricted by the high conformal contact condition. But the sample linearization relationship is not rigorous to describe contact pressure and penetration depth. As shown in Fig. 4, the contact boundary should be a continuous curve, revealing the nonlinear relationship between contact pressure and penetration depth. So a sound relationship between contact pressure and penetration depth should be presented to conduct wear analysis of clearance joint.

On the other hand, the contact force is described as the product of nonlinear power function of penetration depth and contact stiffness in Hertz contact theory. However, it focuses on the spherical contact problems, which focuses on non-conformal contact condition. Hertz contact theory is incorrect when the joint clearance is small. Thus, the application of classic Hertz contact theory is restricted in revolute joint with clearance. The most important thing for Hertz contact theory is to solve the conformal contact problem.

According to the analysis above, the nonlinear contact pressure distribution model is presented in this paper. The bushing is taken as a simple Winkler elastic foundation. The discrete thought of Winkler model is adopted to deal with contact problem with a high conformal rate. Then, we divide the contact area into

Fig. 3 Comparison between Winkler model and asymmetric Winkler model. **a** Traditional Winkler model and **b** asymmetric Winkler model

Fig. 4 Actual contact boundary of Winkler model

many small parts, until the curvature of each small part can be regardless. That is to say, each small part can be seen as a plane. The contact relationship in a local microcontact area can be regarded as the contact between cylinder and plane. And the local contact pressure is acquired based on Hertz contact force model. The NLCP model has not only described the nonlinear relationship between contact pressure and penetration depth, but also avoided the complexity in contact pressure computation.

The relationship between contact pressure and penetration depth is described as follows.

$$\begin{cases} p_i = K\delta_i^n / A_i \\ F_{\text{total}} = \sum_{i=1}^{N} p_i A_i \cos \beta_i \end{cases} \qquad (7)$$

where p_i—contact pressure; K—contact stiffness coefficient, calculated by Eq. (2); n—the nonlinear power exponent determined from material and geometric properties of the local region of the contacting objects [13,17]; δ_i—relative penetration depth; A_i—contact area at the ith spring; F_{total}—total pressure of all the springs; β_i—angle between the ith spring and external load; and N—total spring number in contact area.

The algorithm flowchart of NLCP model is shown in Fig. 5. The detailed processes are as follows:

1. The penetration depth of compression center is assumed as δ_i.
2. Given the non-circular characteristic of inner surface caused during the wear process, the arc function is no longer appropriate to calculate the number of compression springs on each side. According to the boundary conditions of deformation edge, the discrete geometry data of pin surface and bushing
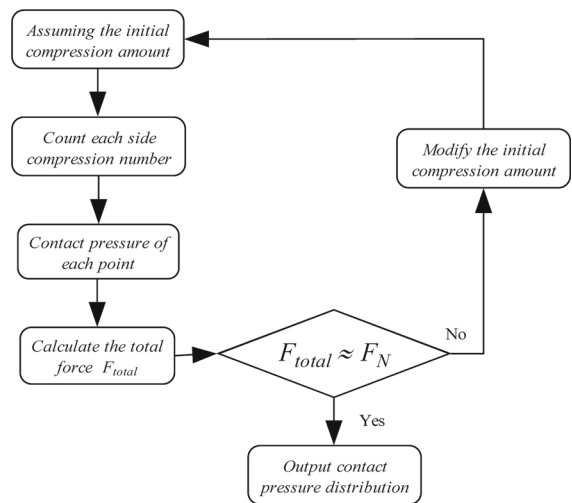

Fig. 5 Algorithm flowchart of NLCP model

inner surface are adopted to calculate the number of compression springs on both sides in this algorithm.
3. According to the number and the penetration depth of compression springs, the contact pressure distribution of contact surface is obtained.
4. Compute the resultant force of compression springs F_{total}. If the resultant force F_{total} is equal to the contact force F_N, i.e., when the difference between F_{total} and F_N is less than 1×10^{-12}, the contact pressure distribution is output. Or, return to the first step. Modify the initial penetration depth δ_i, where the adaptive method is adopted to obtain a better δ_i, and continue iterating, until they are balanced.

3 Analysis of simulation and experiment

3.1 Simulation analysis

The wear behavior is the prominent characteristic of dynamics analysis with clearance. Thus, the wear condition analysis is taken as an evaluation criterion to make comparison with different contact models. The most frequently used model is based on the Archard's wear model [31,32]. It is assumed that wear can be evaluated by applying Archard's equation to local contact conditions along a differential width of the contact interface [33]. The Archard's wear calculation formula is described as follows [34]:

$$V = k\frac{F_N s}{H} \tag{8}$$

where V—wear volume; k—dimensionless wear coefficient; F_N—external load; H—brinell hardness; and s—relative slippage distance of contact surface.

Because the normal penetration depth is considered more in engineering practice, take the differential of contact area in Eq. (8) on both sides.

$$h = k\frac{ps}{H} = K_d ps \tag{9}$$

where h—normal wear depth; p—contact pressure, obtained by Eq. (7); K_d—linear wear coefficient, obtained by wear test of pin–disk pairs; and s—relative slippage distance of contact surface [8]. The slippage distance is the relative movement distance of pin and bushing in the circumferential direction. According to the change size of azimuth of the adjacent contact pressure and the structure data of bushing inner surface, the relative slippage can be obtained. After the bushing contour is updated, the azimuth of contact force and the structure of bushing inner surface will be also changed. Then, the slippage distance will be correspondingly updated.

The wear process can be treated as a dynamic process depending on many parameters, and the prediction of that process can be treated as an initial value problem. As shown in Fig. 6, the impact within a revolute clearance joint in a basic slider–crank mechanism is regarded as an example to compare different contact models. The massless linkage model is adopted to conduct dynamics analysis. The joint clearance is substituted by a massless rod CD. The length of AB, BC and CD is l_1, l_2, ξ. The azimuth of AB, BC and CD is $\varphi_1, \varphi_2, \gamma$. The mass of crank, linkage and slider is
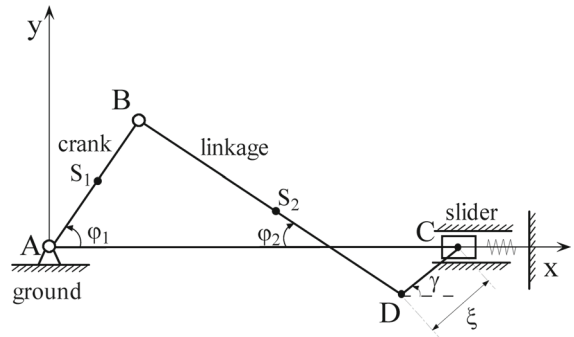

Fig. 6 Slider–crank mechanism with clearance joint

Table 1 Basic parameters of slider–crank mechanism

m_1	m_2	m_3	l_1	l_2	K_s
0.46 g	1.09 g	5 g	0.07 mm	0.2 mm	1800 N/m

Table 2 Basic parameters of clearance joint

	Radius (mm)	Material	E	ν	K_d
Pin	7.45e−3	Steel	2.09e11	0.28	–
Bushing	7.5e−3	PTEF	5.00e08	0.38	5.05e13

m_1, m_2, m_3. To ensure that the pin and bushing are always in contact during the operation process, a spring system is attached to the right of this machinery. The elasticity coefficient of spring is K_s. Assuming that the crank rotates at a constant speed, the angular velocity is ω. The initial clearance size is e. The basic parameters of the slider–crank mechanism and clearance joint are shown in Tables 1 and 2.

The machinery location constraint equations:

$$\begin{cases} l_1 \cos\varphi_1 + l_2 \cos\varphi_2 + \xi\cos\gamma = x_3 \\ l_1 \sin\varphi_1 - l_2 \sin\varphi_2 + \xi\sin\gamma = 0 \end{cases} \tag{10}$$

The machinery dynamics constraint equations:

$$\begin{cases} F_x = F_{k\_\text{spring}} - m_3\ddot{x}_3 \\ F_y l_2 \sin\phi_2 + F_x l_2 \cos\phi_2 - I_2\ddot{\phi}_2 \\ \quad -\frac{1}{2}m_2 l_2 \left[(g + \ddot{y}_2)\cos\phi_2 + \ddot{x}_2 \sin\phi_2\right] = 0 \end{cases} \tag{11}$$

where I_2—rotational inertia of BD.

The massless model is based on continuous contact hypothesis, and the azimuth of contact force is regarded as equal to the azimuth of ideal contact force. Therefore, the solving process of nonlinear dynamics equations can be greatly simplified. Through solving the standard slider–crank mechanism without clearance,

the azimuth of ideal contact force is obtained, i.e., the value of γ. Then, solving Eqs. (10) and (11), F_x and F_y can be obtained.

$$F_N = \sqrt{F_x^2 + F_y^2} \qquad (12)$$

where F_N—the contact force.

In dynamic analysis of multi-body systems with collisions, the deformation is known at every time step from the configuration of the system and the forces are evaluated based on the state variables. With the variation of the contact force during the contact period, the dynamic system's response is obtained by simply including updated forces into the equations of motion. As the equations of motion are integrated over the period of contact, the wear results are calculated in a rather accurate response. According to the analysis of the references [24,25], it is obvious that the contact pressure obtained by the Winkler model turns out to be more effective than the Hertz theory. So a comparison between NLCP model and Winkler mode is presented to verify the correctness of NLCP model. The detailed analysis flowchart of this paper is shown in Fig. 7.

Firstly, the dynamics analysis is performed based on massless model. The contact force and corresponding azimuth of contact force can be obtained by solving Eqs. (10)–(12). Secondly, based on the NLCP model or Winkler model, the contact pressure distribution is calculated. With the contact pressure and corresponding relative slippage distance, the Archard model is used to conduct wear calculation. Then, according to the wear results of every wear cycle, the bushing contour is updated. By repeating the above process continuously, the final wear results are obtained.

Through dynamics analysis, the wear results with different contact pressure calculation models are exhibited in Figs. 8, 9, 10, 11 and 12. Figures 8, 9 and 10 are the wear results in a single wear cycle. The wear results are magnified 1000 times. Figures 11 and 12 are the wear results in many wear cycles.

From Figs. 8 and 9, we can see that the wear results of NLCP model agree with the wear results of asymmetric Winkler model well at different rotation speeds. From Figs. 9 and 10, we can see that the wear results of NLCP model also agree with the wear results of asymmetric Winkler model well with different initial clearances.

As shown in Table 3, the main wear data at different rotation speeds are displayed. The wear peak and wear mass are magnified 1000 times. The NLCP model has wider wear width and weightier wear mass than asym-
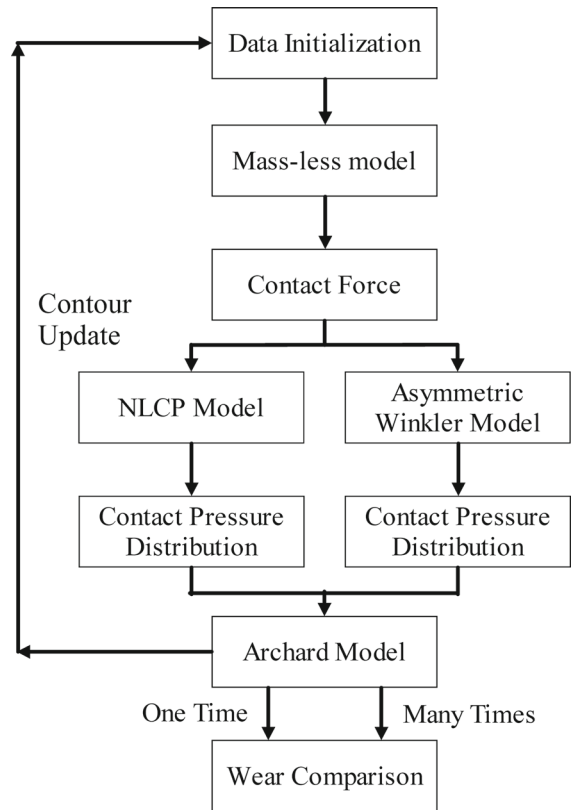

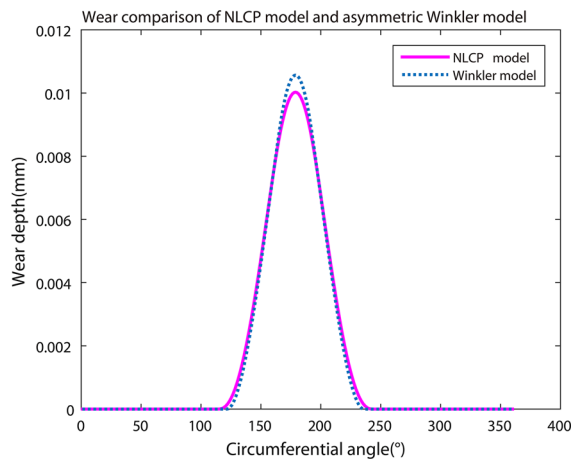**Fig. 7** Analysis flowchart of this paper

Fig. 8 Wear comparison of NLCP model and asymmetric Winkler model (120 rpm, 0.05 mm)

metric Winkler model. Meanwhile, the NLCP has a lower wear peak than asymmetric Winkler model. As shown in Table 4, the main wear data with different initial clearances are displayed. The wear peak and wear
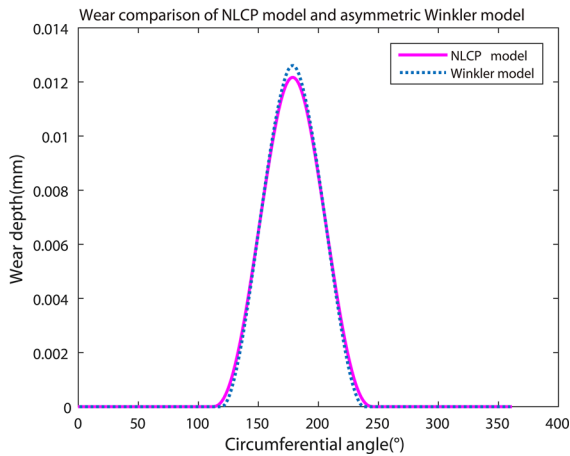
Fig. 9 Wear comparison between NLCP model and asymmetric Winkler model (240 rpm, 0.05 mm)
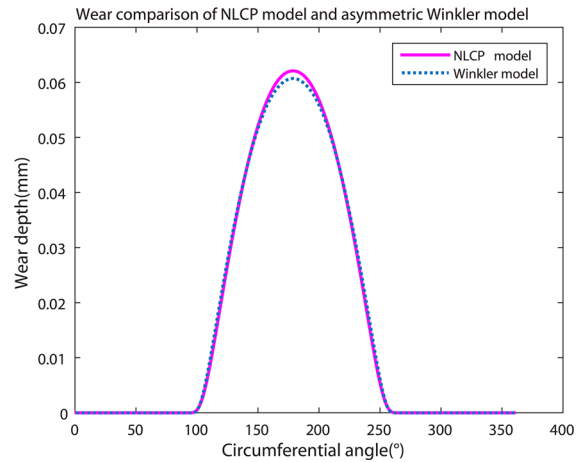

Fig. 11 Wear comparison between NLCP model and asymmetric Winkler model (10000 r, 120 rpm, 0.05 mm)
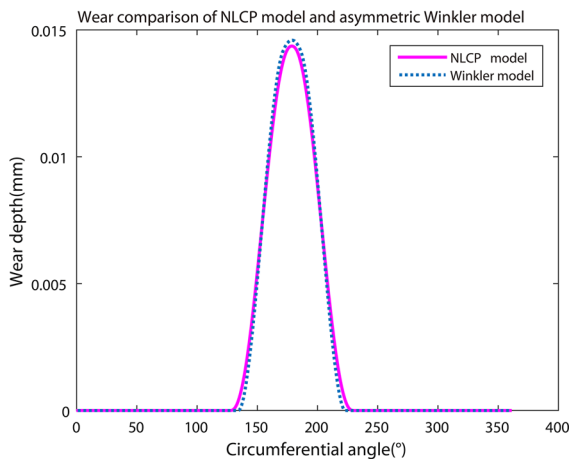

Fig. 10 Wear comparison between NLCP model and asymmetric Winkler model (240 rpm, 0.2 mm)
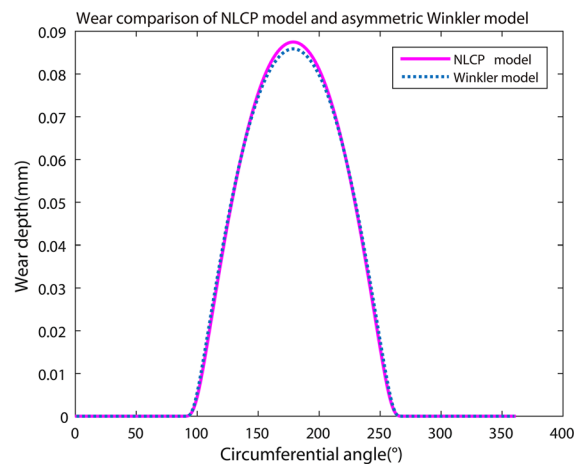

Fig. 12 Wear comparison between NLCP model and asymmetric Winkler model (15000 r, 120 rpm, 0.05 mm)

mass are magnified 1000 times. A similar wear trend with Table 3 can be found. Because of the nonlinear relationship between contact pressure and penetration depth in NLCP model, it will cause a wider deformation region than asymmetric Winkler model with the same contact force. As a result, the penetration depth of compression center is relatively small. The contact pressure of compression center is relatively small. The wear peak is small in a single wear cycle. In addition, the running time of both models has a small difference, revealing the NLCP model has a good efficiency.

In order to fully verify the correctness of NLCP model, a further wear research is conducted as shown in Figs. 11 and 12. The detailed wear results in many

wear cycles are as shown in Table 5. It's obvious to find that the NLCP model has larger wear peak and wider wear width and weightier wear mass than asymmetric Winkler model in a long revolution times. As mentioned above, the contact pressure with the same penetration depth is smaller in NLCP model than that in asymmetric Winkler model. The NLCP model has a relative wide contact area with the same contact force. Thus the wear width of NLCP model is relative wide. Meanwhile, because the large wear area caused by the same contact force, the contact numbers of wear peak position are relatively increased in a continuous contact process between pin and bushing. The more the contact numbers, the heavier the wear condition. Conse-

Table 3 Wear results comparison between NLCP model and asymmetric Winkler model

Model	Time (s)	Rotation speed (rpm)	Wear peak (mm)	Wear width (°)	Wear mass (g)
NLCP	2.11	120	1.003e−5	130	3.381e−6
	1.81	240	1.22e−5	134	4.357e−6
Winkler	2.12	120	1.056e−5	115	3.355e−6
	1.61	240	1.26e−5	118	4.326e−6

Table 4 Wear results comparison between NLCP model and asymmetric Winkler model

Model	Time (s)	Initial clearance (mm)	Wear peak (mm)	Wear width (°)	Wear mass (g)
NLCP	1.81	0.05	1.22e−5	134	4.357e−6
	1.68	0.2	1.44e−5	102	4.23e−6
Winkler	1.61	0.05	1.26e−5	118	4.326e−6
	1.34	0.2	1.46e−5	90	4.21e−6

Table 5 Wear results comparison between NLCP model and asymmetric Winkler model

Model	Time (s)	Revolution number (r)	Wear peak (mm)	Wear width (°)	Wear mass (g)
NLCP	19.81	10000	0.062	169	0.0354
	29.03	15000	0.0875	178	0.0539
Winkler	14.12	10000	0.061	165	0.0353
	21.09	15000	0.0859	176	0.0538

quently, the wear peak in NLCP model is relative larger than that in asymmetric Winkler model under the same conditions. Otherwise, the running time in Table 5 of NLCP model is tolerable in engineering applications, revealing a good efficiency.

In order to analyze the wear behavior due to geometry evolution based on NLCP model, several researches are conducted as shown in Figs. 13, 14 and 15. From Fig. 13, if the bushing contour did not update during the wear process, we can find that the wear results are proportional to the increase of wear cycles. Moreover, the wear areas are the same in different wear cycles. However, as shown in Fig. 14, the bushing contour is updated according to the wear results in corresponding wear cycle in NLCP model. With the increase of wear cycles, the wear area expands in both sides. Meanwhile, comparing with Fig. 13, it is noticeable that the wear peak in Fig. 14 is smaller than that in Fig. 13 with the same wear cycle, which is true with the real wear situation. When the wear behavior happens, the bushing contour changes with material loss and is no longer a
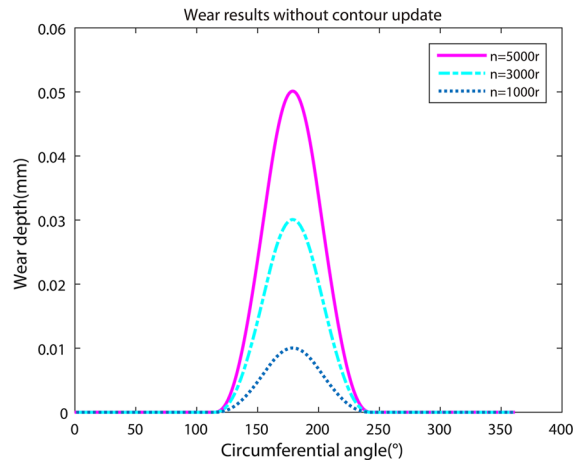

Fig. 13 Wear results without contour update (0.05 mm, 120 rpm)

standard circle. Then, the real contact area will change large and is no lager the same with the initial contact area. The larger the contact area, the larger the wear area. Consequently, the wear area becomes large with
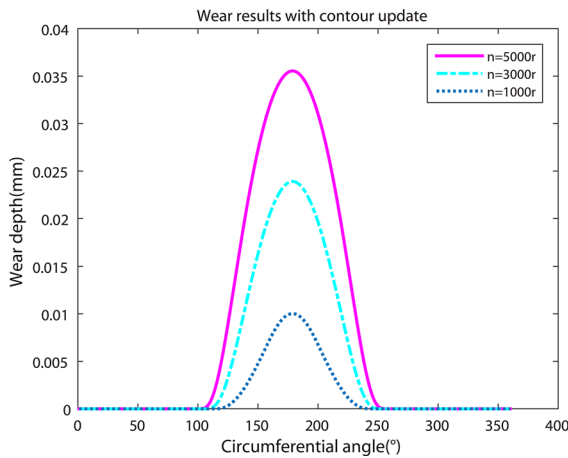
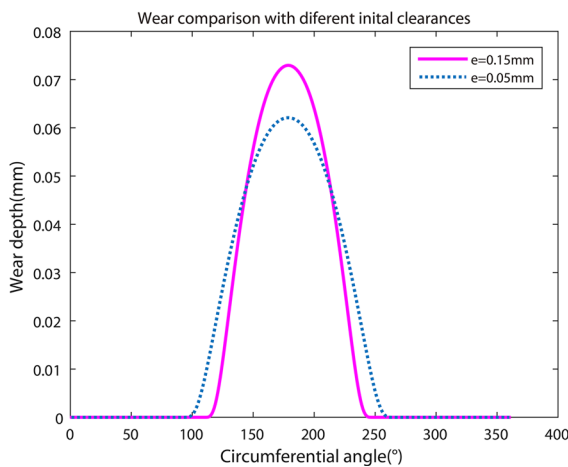**Fig. 14** Wear results with contour update (0.05 mm, 120 rpm)

Fig. 15 Wear results with different initial clearances (120 rpm, 10000 r)

the increase of wear cycles. Considering the contact area becomes large, the contact pressure of contact center will become small, that is why the wear peak will become small when the bushing contour is updated. Overall, the material loss has a big influence on the contact pressure distribution and wear behavior of the system.

Through changing the geometry characteristic of bushing inner surface, the wear results with different initial clearance are obtained, as shown in Fig. 15. At the same rotation speed and in the same wear cycles, when the initial clearance increases, the wear peak becomes large and the wear mass becomes weighty. However, the wear width becomes small. Therefore,

the geometry characteristic will affect the wear results a lot.

Otherwise, the material properties of the contact surfaces also contributed to the wear behavior, such as the surface texture. In terms of the contact stiffness coefficient defined in this paper, it is a simplified calculation method defined by Hertz model. In fact, the contact stiffness coefficient should be nonlinear, which relates to material property, geometry property, clearance size and deformation of contact bodies, as described by Bai and Zhao [19]. It varies with the penetration depth and is not constant during the contact process. The nonlinear stiffness coefficient should be found as the slope of the load–displacement relationship curve by improved elastic foundation model around the point of instantaneous deformation, which will be further studied in the future work.

3.2 Experiment validation

The schematic of slider–crank mechanism is shown in Fig. 16, and the actual experimental device of slider–crank mechanism is shown in Fig. 17. The test device is driven by AC electrical motor, and the rotation speed is controlled by the inverter. The counter is used to measure the rotation times. The test bushing is mounted in the joint between linkage and slider where clearance exists, and the other movement pairs are regarded as ideal joints. The initialization data of this mechanism are shown in Tables 1 and 2.

A series of experiments were conducted to verify the correctness of NLCP model. The coordinates of bushing inner surface are measured by the optical image measuring instrument. The detailed collection process of experimental data is as follows.

1. Measure the coordinates of bushing inner surface;
2. Calculate the coordinates of bushing center by the least squares method;
3. Calculate the distances between bushing center and each point on the bushing inner surface, then minus the initial radius of busing; as a result, the wear amount of busing inner surface is obtained;
4. Collate the experimental data and make comparison with simulation data.

As shown in Figs. 18, 19 and 20, several comparisons between experimental data and simulation data under different conditions are presented.

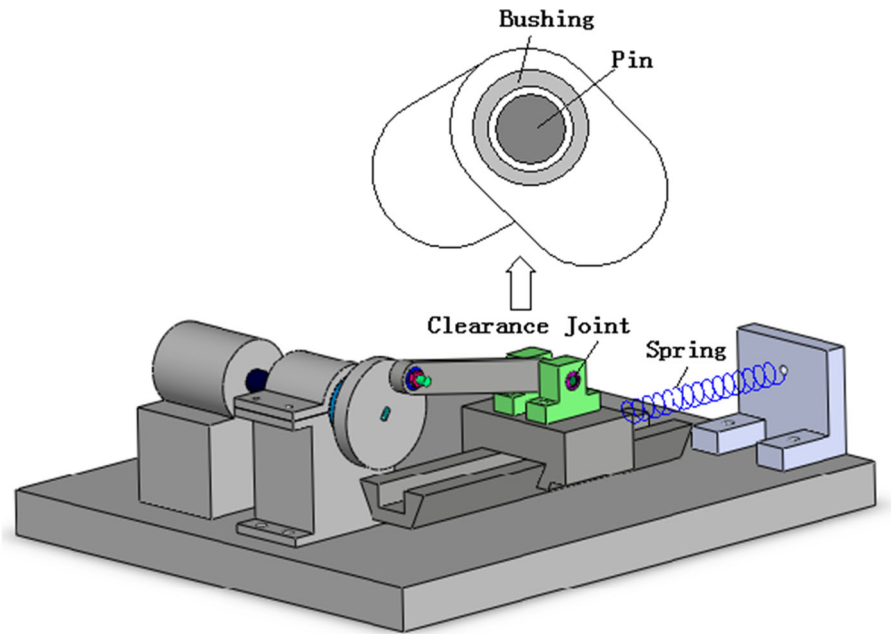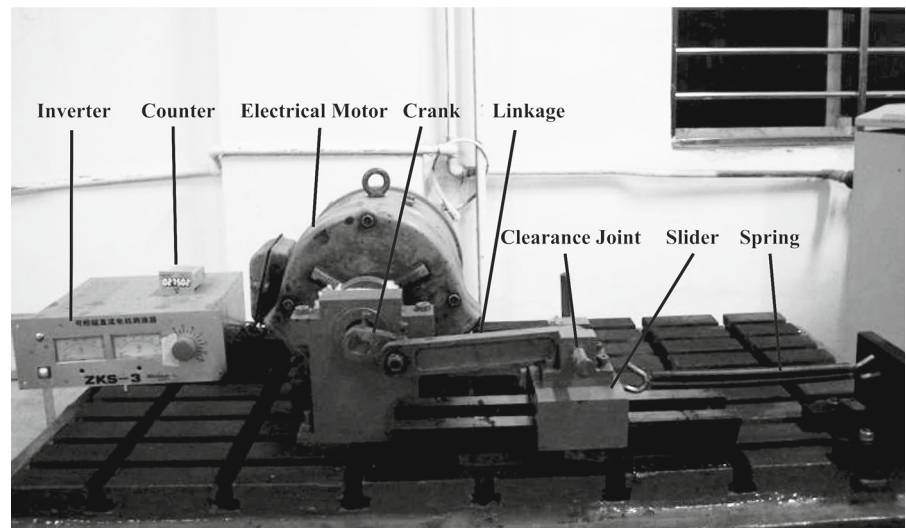**Fig. 16** Schematic of slider–crank mechanism

Fig. 17 Actual experimental device of slider–crank mechanism

Based on the comparison between experimental data and simulation data under different conditions, the calculation results of NLCP model agree with the experimental results. Additionally, several conclusions can be obtained as follows.

1. When the rotation speed increases, the wear peak becomes large, the wear width becomes wide, and the wear mass becomes weighty.
2. When the initial clearance increases, the wear peak becomes large and the wear mass becomes weighty. However, the wear width becomes small.

3. When the revolution times increase, the wear peak becomes large, the wear width becomes wide, and the wear mass becomes weighty.

In summary, considering the other movement pairs in crank–slider mechanism are not ideal, and the small changes of rotation speed caused by voltage fluctuation, and the effect of friction in clearance joint, the deviations cannot be avoided. Although there are few deviations between experimental results and simulation results, the NLCP model still shows a good match with experimental results. Therefore, through a comprehen-
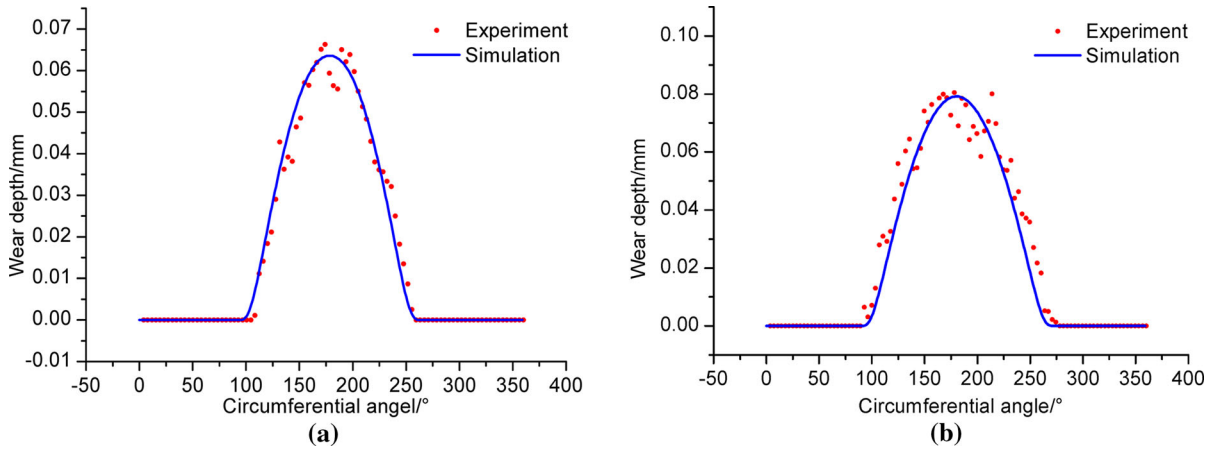
Fig. 18 Comparison between experimental data and simulation data at different rotation speeds. (a 148rpm b 276rpm)
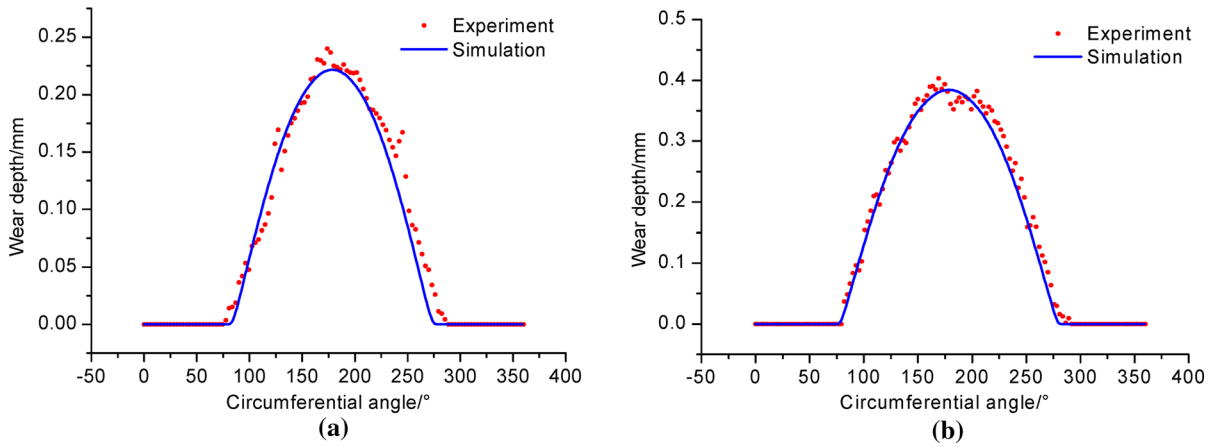

Fig. 19 Comparison between experimental data and simulation data with different initial clearances. (a 0.05 mm b 0.15 mm)
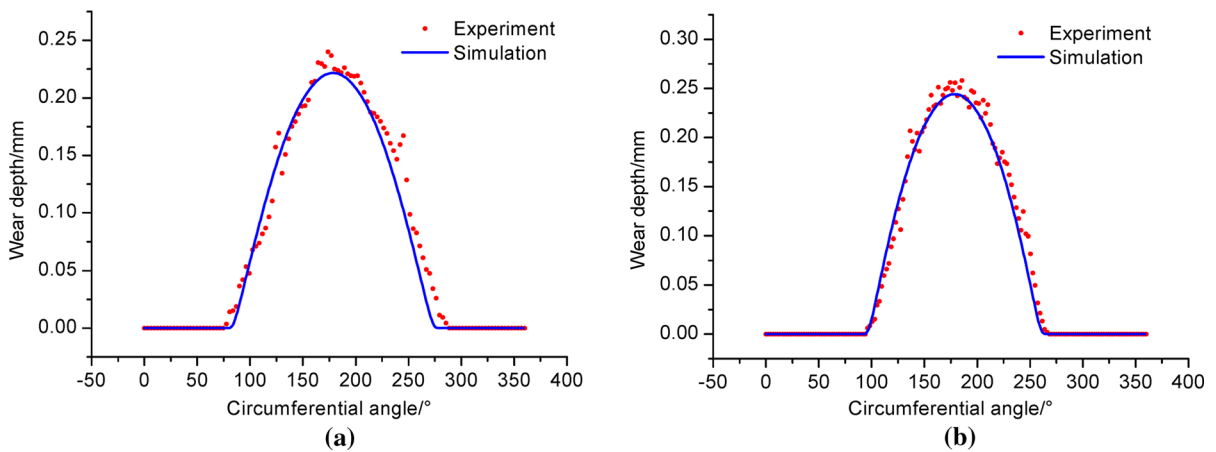

Fig. 20 Comparison between experimental data and simulation data in different wear cycles. (a 40000r b 70000r)

sive experimental study discussed above, the correctness of NLCP model is verified. In short, the NLCP model has enhanced the calculation accuracy with a good efficiency.

4 Conclusions

The wear analysis of clearance joint is a complex engineering problem with the coupling and interaction of multi-body dynamics and tribology. As the key part to conduct coupling analysis of tribology and dynamics of clearance joint, the contact pressure distribution model is studied by many scholars. In order to improve the calculation accuracy of traditional Winkler model and to ensure a good efficiency, the NLCP model is proposed in this paper. The discrete thought of Winkler model is adopted to deal with contact problem with a high conformal rate. The contact relationship in a local microcontact area can be regarded as the contact between cylinder and plane. And the local contact pressure is acquired based on Hertz contact theory. The NLCP model has not only described the nonlinear relationship between contact pressure and penetration depth, but also avoided the complexity in contact pressure computation. The performance of NLCP model is demonstrated in comparison with asymmetric Winkler model, revealing that NLCP model has enhanced the calculation accuracy with a good efficiency. A comprehensive experimental study on the wear calculation of a slider–crank mechanism with clearance joint is presented and discussed to provide an experimental verification for NLCP model.

Additionally, based on the NLCP model, the influence of geometry characteristic on wear behavior is studied. Through updating the bushing contour, the wear area expands in both sides and the wear peak becomes small. The contact force model must consider the material and geometric properties of the contact surfaces, consider information on the impact velocity and contribute to an efficient integration. These characteristics will be ensured with the improved contact force model in the future work. Extensive work will be conducted to improve the NLCP model in the future. Overall, the paper's work has solved the contact problem with a high conformal rate and has described the nonlinear relationship between contact pressure and penetration depth. It has great value to the wear analysis of clearance joint.

References

1. Erkaya, S., Uzmay, I.: Investigation on effect of joint clearance on dynamics of four-bar mechanism. Nonlinear Dyn. **58**(1), 179–198 (2009)
2. Flores, P., Leine, R., Glocker, C.: Modeling and analysis of planar rigid multibody systems with translational clearance joints based on the non-smooth dynamics approach. Multibody Syst. Dyn. **23**(23), 165–190 (2010)
3. Flores, P., Koshy, C.S., Lankarani, H.M., et al.: Numerical and experimental investigation on multibody systems with revolute clearance joints. Nonlinear Dyn. **65**(4), 383–398 (2011)
4. Askari, E., Flores, P., Dabirrahmani, D., et al.: Nonlinear vibration and dynamics of ceramic on ceramic artificial hip joints: a spatial multibody modeling. Nonlinear Dyn. **76**(2), 1–13 (2014)
5. Tian, Q., Liu, C., Machado, M., et al.: A new model for dry and lubricated cylindrical joints with clearance in spatial flexible multibody systems. Nonlinear Dyn. **64**(1), 25–47 (2011)
6. Erkaya, S., Uzmay, I.: Effects of balancing and link flexibility on dynamics of a planar mechanism having joint clearance. Sci. Iran. **19**(3), 483–490 (2012)
7. Pereira, C.M., Ramalho, A.L., Ambrosio, J.A.: An enhanced cylindrical contact force model. Multibody Syst. Dyn. **35**(3), 277–298 (2015)
8. Askari, E., Flores, P., Dabirrahmani, D., et al.: Dynamic modeling and analysis of wear in spatial hard-on-hard couple hip replacements using multibody systems methodologies. Nonlinear Dyn. **82**(1–2), 1039–1058 (2015)
9. Yaqubi, S., Dardel, M., Daniali, H.M., et al.: Modeling and control of crank-slider mechanism with multiple clearance joints. Multibody Syst. Dyn. **36**(2), 1–25 (2015)
10. Varedi-Koulaei, S.M., Daniali, H.M., Farajtabar, M., et al.: Reducing the undesirable effects of joints clearance on the behavior of the planar 3-RRR parallel manipulators. Nonlinear Dyn. **86**(2), 1–16 (2016)
11. Askari, E., Flores, P., Dabirrahmani, D., et al.: A computational analysis of squeaking hip prostheses. J. Comput. Nonlinear Dyn. **10**(2), 024502 (2014)
12. Johnson, K.L., Johnsonm, K.L.: Contact Mechanics. Cambridge University Press, Cambridge (1987)
13. Machado, M., Moreira, P., Flores, P., et al.: Compliant contact force models in multibody dynamics: evolution of the Hertz contact theory. Mech. Mach. Theory **53**, 99–121 (2012)
14. Ma, J., Qian, L., Chen, G.: Parameter estimation of the Lankarani–Nikravesh contact force model using a new modified linear method. In: IEEE International Conference on Advanced Intelligent Mechatronics. IEEE (2015)
15. Hunt, K.H., Crossley, F.R.E.: Coefficient of restitution interpreted as damping in vibroimpact. J. Appl. Mech. **42**(2), 440–445 (1975)

16. Herbert, R.G., Mcwhannell, D.C.: Shape and frequency composition of pulses from an impact pair. J. Eng. Ind. **99**(3), 663–671 (1977)

17. Lankarani, H.M., Nikravesh, P.E.: A contact force model with hysteresis damping for impact analysis of multibody systems. J. Mech. Des. **112**(3), 369–376 (1990)

18. Lankarani, H.M., Nikravesh, P.E.: Continuous contact force models for impact analysis in multibody systems. Nonlinear Dyn. **5**(2), 193–207 (1994)

19. Bai, Z., Zhao, Y.: A hybrid contact force model of revolute joint with clearance for planar mechanical systems. Int. J. Non Linear Mech. **48**(48), 15–36 (2013)

20. Muvengei, O., Kihiu, J., Ikua, B.: Dynamic analysis of planar rigid-body mechanical systems with two-clearance revolute joints. Nonlinear Dyn. **73**(1–2), 259–273 (2013)

21. Zhang, X., Zhang, X., Chen, Z.: Dynamic analysis of a 3-RRR parallel mechanism with multiple clearance joints. Mech. Mach. Theory **78**(78), 105–115 (2014)

22. Pereira, C.M., Ramalho, A.L., Ambrósio, J.A.: A critical overview of internal and external cylinder contact force models. Nonlinear Dyn. **63**(4), 681–697 (2011)

23. Flodin, A., Andersson, S.: Simulation of mild wear in spur gears. Wear **207**(1–2), 16–23 (1997)

24. Põdra, P., Andersson, S.: Wear simulation with the Winkler surface model. Wear **207**(1), 79–85 (1997)

25. Liu, C.S., Zhang, K., Yang, R.: The FEM analysis and approximate model for cylindrical joints with clearances. Mech. Mach. Theory **42**(2), 183–197 (2007)

26. Su, Y., Chen, W., Guo, C.: Wear prediction of clearance revolute joints using winkler surface model. Mocaxue Xuebao/Tribology **32**(4), 320–324 (2012). http://www.tribology.com.cn/ch/reader/create_pdf.aspx?file_no=20120402&year_id=2012&quarter_id=4&falg=1

27. Li, P., Chen, W., Zhu, A.: An improved practical model for wear prediction of revolute clearance joints in crank slider mechanisms. Sci. China Technol. Sci. **56**(12), 2953–2963 (2013)

28. Flores, P., Sio, J., Claro, J., et al.: Influence of the contact-impact force model on the dynamic response of multi-body systems. Proc. Inst. Mech. Eng. Part K J. Multibody Dyn. **220**(1), 21–34 (2006)

29. Hertz, H.: On the contact of solids—on the contact of rigid elastic solids and on hardness (Translated by DE Jones and GA Schott). Miscellaneous Papers (1896)

30. Goldsmith, W., Frasier, J.T.: Impact: the theory and physical behavior of colliding solids. J. Appl. Mech. **28**, 639 (1961)

31. Bai, Z.F., Zhao, Y., Chen, J.: Dynamics analysis of planar mechanical system considering revolute clearance joint wear. Tribol. Int. **64**(3), 85–95 (2013)

32. Flores, P.: Modeling and simulation of wear in revolute clearance joints in multibody systems. Mech. Mach. Theory **44**(6), 1211–1222 (2009)

33. Shen, X., Cao, L., Li, R.: Numerical simulation of sliding wear based on Archard model. In: International Conference on Mechanic Automation and Control Engineering, pp. 325–329 (2010). doi:10.1109/MACE.2010.5535855

34. Archard, J.F.: Contact and rubbing of flat surfaces. J. Appl. Phys. **24**(8), 981–988 (1953)